Veröffentlichung

Autoren

Burnazzi, Marco;Radespiel, Rolf

Titel

SYNERGIES OF SUCTION AND BLOWING FOR ACTIVE HIGH-LIFT FLAPS

Publisher o. Konferenz

DLRK 2013 - German Aerospace Congress 2013, Stuttgart.

Jahr

2013

Internet-Link (Doi-Nr.)

SYNERGIES OF SUCTION AND BLOWING FOR ACTIVE HIGH-LIFT FLAPS

M. Burnazzi, R. Radespiel, Institute of Fluid Mechanics, Technische Universität Braunschweig, Hermann-Blenk-Str. 37, 38108 Braunschweig, Germany

Abstract

The present work represents an advanced step in the multidisciplinary design of an active high-lift system for commercial aircraft. The airfoil configuration developed within the framework of the Collaborative Research Centre SFB880 is composed of an active Coanda flap and a droopnose device. The power required to implement circulation control is provided by electrically-driven compact compressors, positioned along the wing behind the wingbox. This solution could reduce the additional engine power needed for the active high-lift system. Air is provided to the compact compressors by means of a suction slot located on the suction side of the airfoil, which represents an opportunity to increase the aerodynamic performance of the airfoil. The present work investigates the aerodynamic sensitivities of shape and location of the suction slot, in relation to the high-lift performance of the airfoil and to the total pressure recovery achieved at the end of the suction duct. A significant benefit is achieved by suction and the presented analysis yields physical insight into the flow dynamics around the airfoil.

NOMENCLATURE

C_μ	momentum coefficient of the Coanda jet
v_J	Coanda jet velocity
$\dot{m}_J$	Coanda jet massflow
v_∞	freestream velocity
ρ_∞	freestream density
Ma	Mach number
Re	Reynolds number
P_{T_J}	total pressure inside the jet plenum
P_{T_i}	total pressure at the end of the suction duct
PR	compression ratio
$C_{l,max,bal}$	balanced maximum lift coefficient
$C_{\mu,bal}$	balanced jet momentum coefficient
δ_2	boundary layer momentum thickness
c	airfoil chord length

1. INTRODUCTION

The present study is conducted as subproject of the Collaborative Research Centre SFB880 in Braunschweig. The motivation of the Centre is rooted in the realization that European airports used by commercial airliners are currently operating at rather high capacity. There are two ways to cope with future increases in air traffic: a) to build new major airports and b) to develop technologies for new classes of commercial airplanes that can operate from existing European airports not in use for commercial purposes because of short runways or their proximity to populated areas. This class of airplane will have to be quiet and use very short runways for takeoff and landing, while offering high cruise efficiency as well. Special attention is therefore given to high-lift systems, devices that promise significant flight speed reductions at takeoff and landing. Preliminary design of cruise efficient aircraft states that substantial reductions of runway length are only possible by increasing the maximum lift coefficient by significant factors accompanied by a moderate increase of the installed engine thrust [1]. Another problem is that currently used high-lift systems employ gaps, which are major sources of aerodynamic noise during landing. Both these aspects should be improved by the new technologies that are being developed. In particular, the high lift coefficient needed to allow low flight speeds is obtained by active circulation control. This will also lead to a significant noise reduction if gap-less devices at both the trailing edge and the leading edge of the wing are used. Introducing such new devices in commercial aircraft raises many technological issues. The Collaborative Research Centre SFB880 addresses these issues with multidisciplinary research efforts, which allow to simultaneously deal with different aspects of the development of the system and its integration into the aircraft.

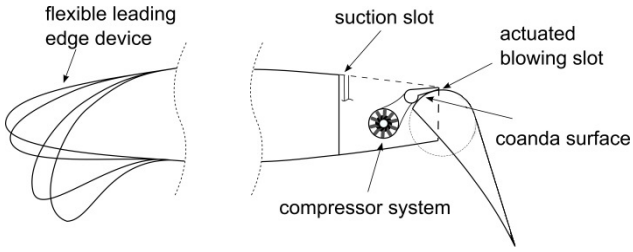

FIGURE 1: High-lift configuration developed by the SFB880 Centre.

The means adopted to provide compressed air to the high-lift device is a set of electric compact compressors integrated into the wing near the flap, as shown in Figure 1. Here aerodynamics plays an important role, as it is responsible for the aerodynamic efficiency of the high-lift system, as well as for providing air to the compact compressors by means of a suction slot located on the suction side at a suited position on the wing. The present work focuses on the design aspects of the suction, based on the following design objectives:

- high lift coefficients and high angles of attack at maximum lift;
- high total pressure recovery at the end of the suction duct.

In order to take into account both objectives, a method is proposed to compare and evaluate the overall performance of the tested geometries.

An important requirement for transport aircraft applications calls for low blowing power of the active control system, as otherwise a significant engine growth will occur compared to using passive high-lift systems. The efficiency of active blowing is usually represented by the lift gain factor, defined as the ratio between the increase of lift coefficient due to the active circulation control system and the jet momentum coefficient needed to obtain this gain. The jet momentum coefficient is given by:

$$C_\mu = \frac{v_J \cdot \dot{m}_J}{\frac{1}{2}\rho_\infty v_\infty^2}$$

where v_J and $\dot{m}_J$ are the velocity and the massflow of the jet through the exit section of the plenum. Quantitative values of lift gain factor had previously not received much attention. Recently, Ref. [2] reviewed the status of published lift gain factors. It was found that the detailed design of blowing slot height, flap angle and Coanda contour along with the blowing rate have a significant impact on the gain factor. Improvements in gain factor can be obtained by using numerical sensitivity investigations to guide the design. Also, extrapolations to flight Reynolds numbers are obtained by numerical flow simulations at low cost relative to experiments.

Recent design data reveal that lift gain factors of around 80 are obtained for active airfoils with maximum lift coefficients of around four and by using steady blowing [3-5]. Note, the gain factor decreases rapidly towards higher lift coefficients. Also, one observes significantly reduced angles of attack for maximum lift at high flap angles and high blowing rates needed to obtain large lift coefficients, i.e. at values around six. It turns out that the suction peak at the airfoil nose generated by the active high-lift flap is responsible for these behaviors. This calls for aerodynamic means to reduce the losses associated with the flow around the leading edge. The solution adopted by the SFB880 is a carefully designed droopnose. This device, associated to an active Coanda flap provides a significantly higher effect than when employed together with a conventional fowler flap [6, 7]. These findings represent the starting point of the present paper.

Chapters 2 and 3 describe the employed high-lift configuration and the numerical approach used for the analysis. Chapter 4 is then a sensitivity study of the effect of different geometrical parameters, which explain the physical principle of the wall suction and the resulting increase of performance. Subsequently the response to different jet momentum coefficients is presented in Chapter 5. In this context wall suction is also applied to the clean nose configuration, showing the higher benefit generated by the new device in presence of the droopnose leading-edge protection. Finally the improvement of aerodynamic coefficients and lift gain factor is reported.

2. HIGH-LIFT CONFIGURATION

The airfoil with high-lift configuration analyzed in the present work, shown in Figure 2, is the DLR F15 airfoil equipped with three high-lift devices:

- Coanda trailing edge flap;
- droopnose leading edge;
- suction slot.

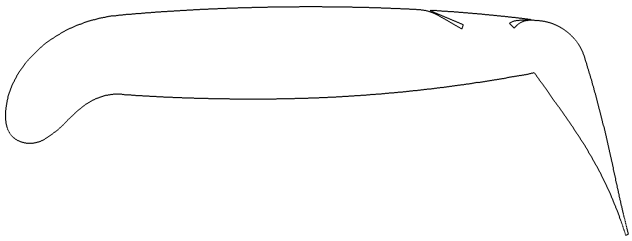

FIGURE 2: Analyzed high-lift configuration

As mentioned above the present study deals with the implementation of the suction slot on the previously designed configuration. Thus, the following sections describe the starting point of the study.

2.1. Trailing-edge device

This section describes previous numerical and experimental flow research aimed at improving the lift gain factor by careful adjustments of the design parameters of the trailing edge device while the leading edge was geometrically fixed. These initial design studies assumed steady blowing to produce suited turbulent wall jets that exploit the Coanda effect for effective flow turning. The most important design parameters are flap deflection angle, momentum coefficient of blowing and blowing slot height [4]. While flap angle and blowing momentum coefficient should increase for increased lift targets, optimal slot heights are rather small, with values of around 0.0006 times the airfoil chord length. Surprisingly, the optimum slot height is independent of the flap angle. Figures 3 and 4 display a typical design result, where the transonic airfoil DLR F15 is equipped with an internally blown flap set at 65° deflection angle.

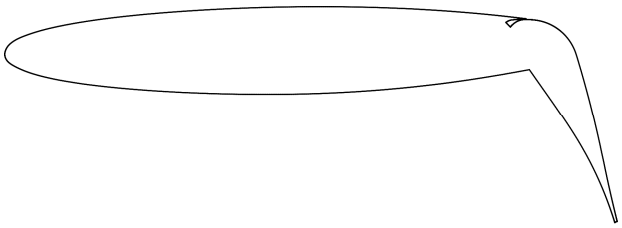

FIGURE 3: DLR F15 airfoil, equipped with active Coanda flap

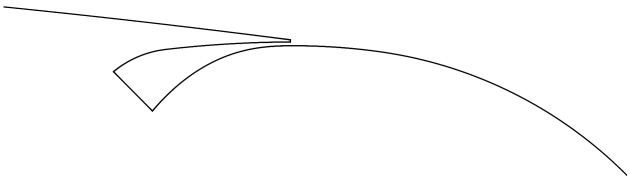

FIGURE 4: Detail of the blowing slot

The detailed curvature distribution of the Coanda surface used as flap knuckle shape was found less important. Values of the radius of curvature of around 0.07 times the chord length are a reasonable design choice. Also the flap length suited to achieve high lift gains could be identified. Best lift gain factors were obtained with flap lengths of 0.25-0.30 times the airfoil chord [3]. With these design choices typical lift gains over blowing momentum (lift gain factor) of 80 are obtained at a lift coefficient around 4 whereas this value is reduced to 55 at a lift coefficient around 6.

These design studies were accompanied by significant efforts to validate the numerical simulations with the RANS solver. Simulations of Coanda wall jets over a blunt trailing edge showed the necessity to augment standard turbulence models with correction terms to take into account streamline curvature effects on turbulent transport [5], similarly as found by Swanson and Rumsey [8]. Airfoil wind tunnel experiments were performed to verify the Coanda flap designs and the results were compared to 3-D flow simulations that included the wind tunnel wall effects [9]. These studies revealed good agreement in terms of maximum lift and the corresponding angle of attack. It was generally noticed though, that the angle of attack of maximum lift reduces significantly at higher blowing rates, as seen in Figure 5 for a typical wind tunnel Reynolds number.

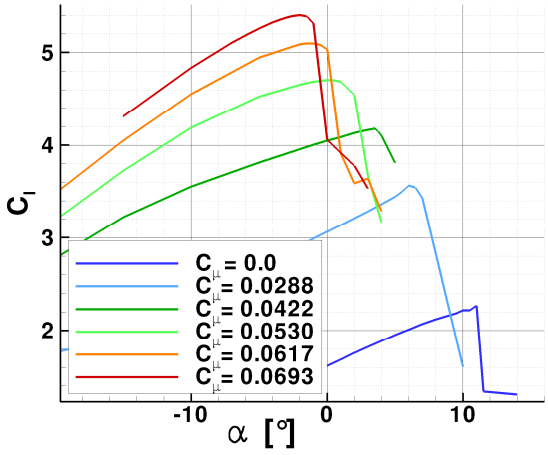

FIGURE 5: Effect of blowing momentum on the angle of maximum lift for the DLR F15 airfoil with 65° flap angle, computed for Ma=0.15, Re=1.7·10^6, according to Ref. [10]

As the adverse pressure gradient along the suction side, downstream of the suction peak at the nose, grows rapidly with the angle of attack it creates significant momentum losses towards the trailing edge device. This adversely affects the ability of the wall jet to provide flow turning. Local blowing at the nose or at other locations of the airfoil did not help much, as it extended the useful angle-of-attack range but generally at the cost of decreasing the lift gain factor [4]. Note that the simulations predicted leading edge stall for the DLR F15 airfoil at lift coefficients above 6.

2.2. Leading-edge device

In order to control the pressure distribution, the shape of the clean nose was morphed. As one can see in Figure 2, the camber-line and the thickness are increased, resulting in a reduction of the suction peak over the nose. The morphed shape allows to distribute the low pressure area on a wider surface, reducing the minimum values. This new load distribution results in different stall behaviors, as explained in [6].

In Figure 6 one can see a comparison between the clean nose and the droopnose configuration. The C_p distributions refer to stall conditions, and result in the coefficients shown in Table 1.

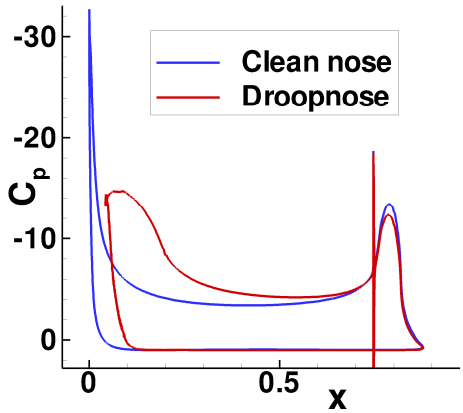

FIGURE 6: C_p distributions at stall conditions, C_μ=0.06

	$C_{l,max}$	$\alpha_{max}[^\circ]$	$C_{d,stall}$	$C_{m,stall}$
Clean nose	5.27	1.5	0.0886	-2.184
Droopnose	6.30	15.0	0.107	-2.44
	+19.5%	+13.5	+20.8%	-11.7%

TABLE 1: Effects due to the droopnose, C_μ=0.06

3. NUMERICAL APPROACH

The present investigations are based on 2D simulations of the DLR F15 airfoil in high-lift configuration. The CFD solver employed to perform the analysis is the DLR TAU-Code [11, 13]. The Reynolds Averaged Navier-Stokes (RANS) equations are solved by using a finite-volume approach. The numerical scheme, turbulence model and parameters have been previously assessed by using wind tunnel experiments [9,13]. In particular the present results are obtained by a central scheme for the mean flow inviscid flux and a second order upwind Roe scheme for the convective turbulent flux. The turbulence model is given by Spalart and Allmaras with a correction due to flow rotation and curvature [14]. This last module allows the one-equation turbulence model to maintain a good accuracy also in regions where the streamlines have a high curvature. This characteristic is fundamental for the simulation of the Coanda phenomenon, which is based on the equilibrium between the inertia forces and the momentum transport in the direction normal to the convex surface [5].

The space discretization is realized by a dual grid, obtained by the solver from the initial one, as provided by the user. This is performed by connecting the center of each cell and allows to use hybrid meshes. The number of grid points has been set using a mesh convergence exercise, based on the Richardson extrapolation. This procedure provides an estimation of the space discretization error and of the minimum number of points that produces results with an acceptable accuracy. The resulting grid is made by about 250000 points and composed of an unstructured grid region and a structured area. The structured grid layer starts from the surfaces and is extended to cover the region where the main viscous phenomena occur. It ensures y^+ lower than 1 near the wall. In the grid plots of Figures 7, 8 and 9 one can see some of the main features of the mesh. An important characteristic of the grid, that makes it suitable for high-lift simulations, is the density of points along the pressure side, as the stagnation point will be situated in this region, and can move quite far from the leading edge. A high amount of points is necessary to properly capture the flow attachment. The structured region is extended over a large area above the flap, in order to accurately capture vortices expected in case of flow separation from the flap. Both the trailing edge and the edge of both slot lips are discretized by means of a local C-block topology, in order to avoid the propagation of high point density into areas where grid points are not needed and could slow down the convergence, see Figure 8.

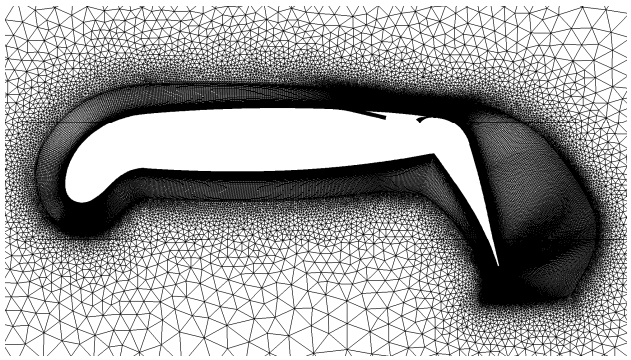

Figure 7: Grid around the whole airfoil

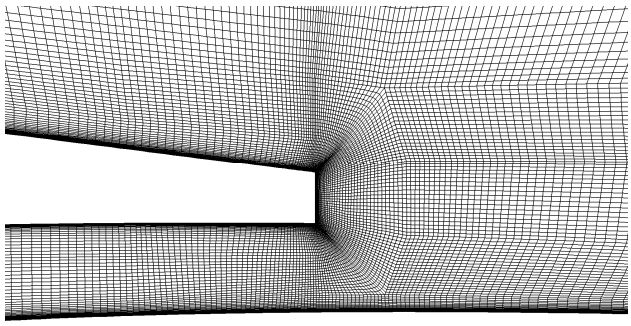

Figure 8: Detail of the grid at the blowing slot

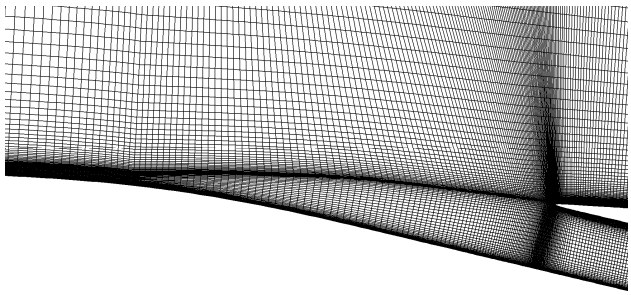

Figure 9: Detail of the grid at the suction slot

4. SENSITIVITY STUDY

The sensitivity study allows to evaluate the effect of wall suction on both the maximum lift coefficient and the total pressure recovery inside the duct. This last quantity is fundamental for the design of the compact compressors, situated downstream of the wingbox, as shown in Figure 1.

Previous analyses, performed with the configuration without suction, drew a clear picture in terms of jet momentum requirements and flow dynamics around the airfoil [6]. For the present study C_μ=0.0356 was chosen, as the flow over the flap results particularly sensitive to the conditions upstream of the flap. With such a blowing rate the jet has just the momentum required to avoid flow separation from the flap, at maximum lift condition. A reduction of the required jet momentum will bring an increase of both the maximum lift and the stall angle of attack. The effect of different blowing rates on the performances and the related flow phenomena, are described in the following Chapter.

The massflow through the suction slot is determined by the jet momentum coefficient and its corresponding massflow. From this value, and the local temperature and density of the outer flow at the suction location, one can estimate the width of the duct needed to obtain a Mach number suited to represent the compressor inlet state. The condition employed in the present work is Ma=0.1, which, for a suction slot located at 61% of the airfoil chord, results in a duct width of about 0.6% of the chord length.

The high-lift configuration used in the present work yields $C_{l,max}$=5.018 at α=12.25°, with Re=12·10^6 and Ma=0.15. For the sensitivity analysis, the angle of attack is fixed at 10°.

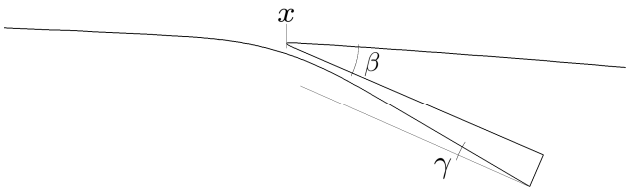

Figure 10: Investigated geometrical parameters

The geometrical parameters varied in the present work are shown in Figure 10. The sensitivity study is structured in two parts: analysis of the internal shape of the duct (β and γ) and study of the suction location (x). In order to compare the overall performance of the tested geometries, the two criteria presented above (maximum lift coefficient and total pressure recovery in the duct) are combined into a single parameter, a balanced lift coefficient, as explained in section 4.3.

4.1. Internal shape analysis

The initial suction location is fixed at 61% of the airfoil chord based on wing structure considerations. This location corresponds to the front edge of the spoiler, and it is downstream of the wingbox (see Figure 1). Positioning the suction slot in the front of the wingbox would involve the duct to pass through the supporting structure of the wing.

As the end section of the duct is fixed by the compressor inlet condition (Ma=0.1), the two geometrical parameters varied in this first step of the analysis are the local duct angle β and the diffusion angle γ, see Figure 10. Minimum value for the angle β is 10°, as lower angles may allow a slightly better pressure recovery inside the duct, but they would also involve a high complexity of construction.

Figure 12 shows the effect of the diffusor angle γ on the lift curve, for a fixed duct angle β=10°. The effects of the wall suction, with respect to the no suction configuration, results in an increase of maximum lift coefficient of about 7%, for the highest diffusion, and of 3° for the corresponding angle of attack.

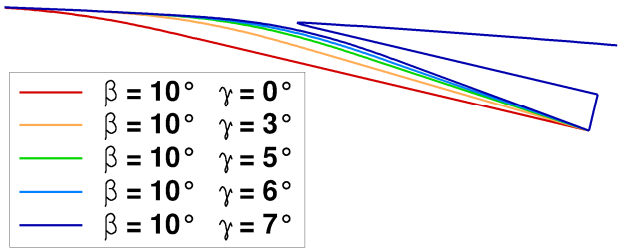

FIGURE 11: Diffusor angle variations for β=10°

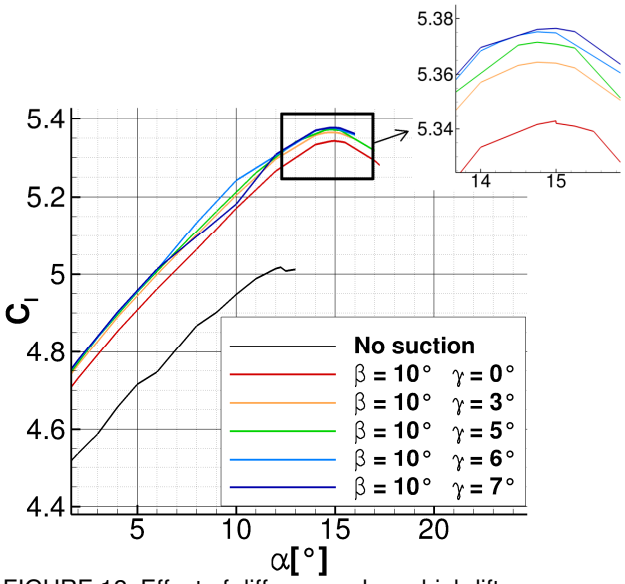

FIGURE 12: Effect of diffusor angle on high-lift performance, for β=10°

With the diffusor angle of 7°, transonic flow in the duct is observed. It appears that such a high angle slightly increases the maximum lift coefficient, without having a significant effect on the stall angle of attack. The lift coefficient increase is about 0.6%, for γ=0°-7° (see Figure 11). Similar variations are obtained by setting the duct angle β=20°: C_l is improved from 5.354 to 5.373 with γ=0°-7°. The influence of the different internal geometries on the total pressure recovery is described in paragraph 4.3, and reported in table 4.

4.2. Location analysis

Once the potentials of the wall suction have been assessed at 61% of the chord length, the suction slot with β=10° and γ=0° is moved to two different locations.

At 30% of the chord length the flow experiences an adverse pressure gradient after the peak in the nose region. This pressure gradient increases the boundary layer thickness, and reduces the momentum of the flow that has to be kept attached to the flap by the Coanda jet. For this reason, the suction of the boundary layer in this area may significantly improve the flow momentum, reducing the required jet momentum coefficient.

The third location is 85% of the chord length. In this area it may be possible to delay the separation from the flap surface for low jet momentum coefficients, when the Coanda jet does not have sufficient momentum to keep

the flow attached until the trailing edge.

Figures 13 and 14 show the airfoil geometry with the suction slot at 30% and 85% of the chord length.

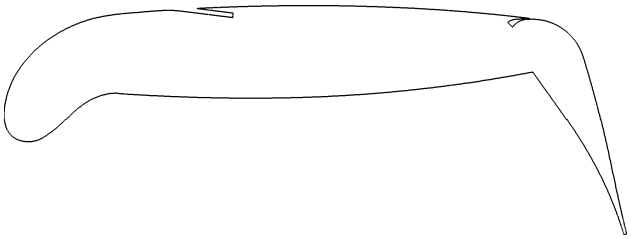

FIGURE 13: Airfoil equipped with wall suction at 30% of the chord length

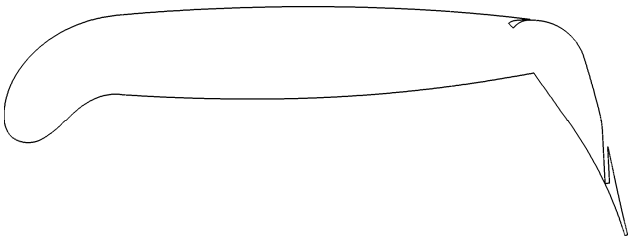

FIGURE 14: Airfoil equipped with wall suction at 85% of the chord length

The location of the suction slot appears to have a higher influence on the aerodynamic performances with respect to the internal shape. With suction at 30%, with respect to the no suction case, C_l is improved by about 12% and the stall angle of attack is increased by 6°. On the other hand, positioning the suction slot on the flap decreases the maximum lift coefficient, as shown in Figure 15. Details about the flow dynamics that rule the performances for the different suction locations are presented in the following.

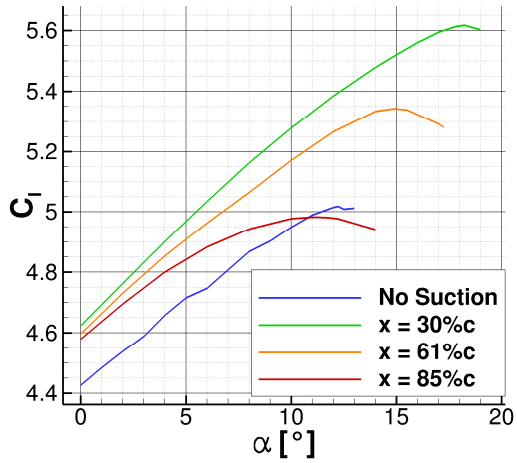

FIGURE 15: Effect of suction location, C_μ=0.0356

4.2.1. Suction at 85%c

The comparison presented in Figure 15 is obtained by C_μ=0.0356, which allows the flow to follow the contour of the flap without separation. In this case a slot positioned on the flap surface reduces the momentum of the boundary layer, sucking part of the Coanda jet. As mentioned above, this suction location might be more effective for lower jet momentum coefficients. For this reason additional computations are conducted with C_μ=0.016. In this case the jet does not have sufficient momentum to keep the outer flow attached until the trailing edge. Unfortunately, as shown in Figure 16, the suction at lower angles of attack is not sufficient to avoid flow separation. Figure 17 shows the effect of suction at stall conditions (17° without suction and 15.25° with suction). At high angles of attack the separation occurs between the jet and the outer flow, which makes the wall suction ineffective. These flow behaviors result in the performances presented in table 2. Details about the stall behavior of the Coanda flap without suction are detailed in [6].

	$C_{l,max}$	α_{stall}
no suction	3.877	17°
suction 85%c	3.82	15.25°

TABLE 2: Effect of suction at 85% of the chord length, C_μ=0.016

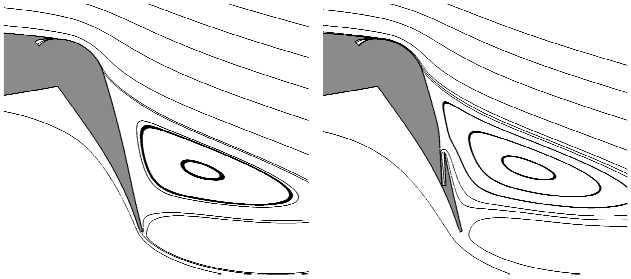

FIGURE 16: Effect of the suction at 85%c on the flow over the flap, C_μ=0.016, α=10°, left without suction, right with suction

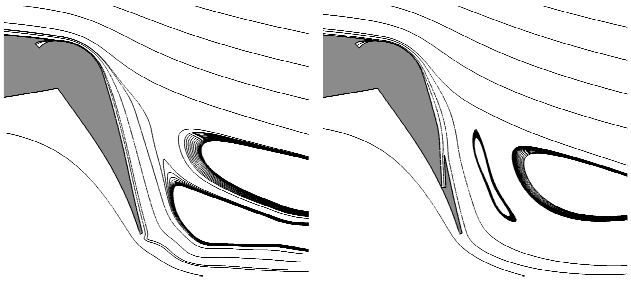

FIGURE 17: Effect of the suction at 85%c on the flow over the flap at stall condition (without suction at 17°, left, and with suction at 15.25°, right), C_μ=0.016

4.2.2. Suction upstream of the Coanda jet

Considering the performance improvement shown in Figure 15, it is worth to investigate more in detail the effect of wall suction upstream of the blowing slot. Contrarily to the suction from the flap surface, both the slot at 30%c and at 61%c reduce the required jet momentum by improving the flow that has to be kept attached to the flap. Figure 18 shows the velocity profiles of the boundary layer just upstream of the blowing slot, as shown by the sketch in the figure. It appears evident that the momentum of the flow in the case of suction at 30% of the chord length is higher than the other cases. Also the values of momentum thickness of the boundary layer at the same location, reported in table 3, confirm the same trend.

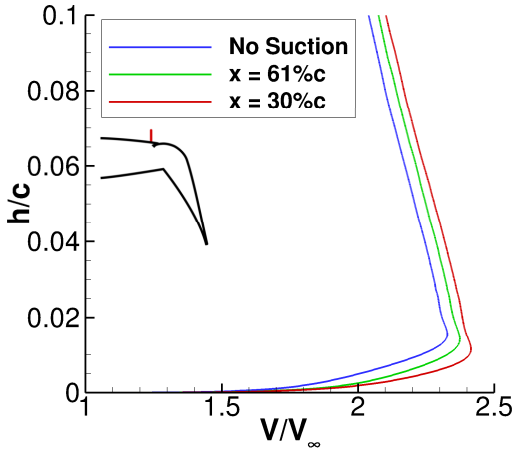

FIGURE 18: Velocity profiles of the boundary layer upstream of the blowing slot, C_μ=0.0356, α=10°

	No Suction	61%c	30%c
δ_2/c	1.29912e-03	9.75340e-04	7.82365e-04

TABLE 3: Boundary layer momentum thickness upstream of the blowing slot, C_μ=0.0356, α=10°

The lower momentum loss of the boundary layer flow in the case of suction at 30%c, causes the overall airfoil flow to obtain higher circulation, increasing also the velocity of the flow over the nose. This is shown in Figure 19, which reports the pressure coefficient distributions for the two suction locations upstream of the Coanda jet, and for the airfoil without suction. The effect of the suction on the pressure distribution appears similar to an increase of jet momentum coefficient, making a reduction of C_μ required to reach a certain lift coefficient possible.

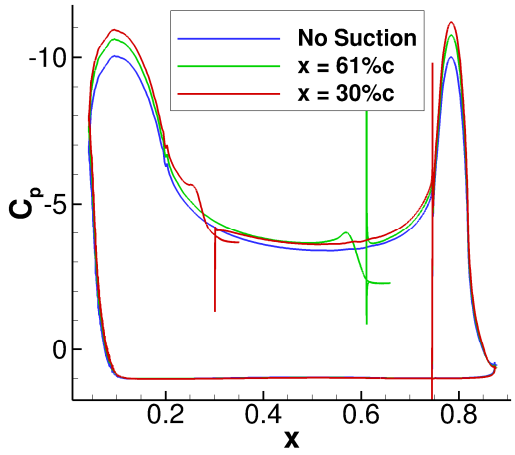

FIGURE 19: C_p distributions for Cμ=0.0356, α=10°

4.3. C_l balance

As mentioned above, the objectives of the wall suction are to provide air with high pressure recovery to the compact compressors and to improve the high-lift capabilities of the airfoil. Unfortunately these two criteria do not follow the same trend for variations of the geometrical parameters. Therefore a combined parameter is needed to compare the actual benefit of the tested geometries. For this purpose the total pressure obtained at the end of the suction duct is used to balance the jet momentum coefficient, by assuming a constant compression ratio of the compressor. This results in a balanced lift coefficient that is used to compare and evaluate different geometries.

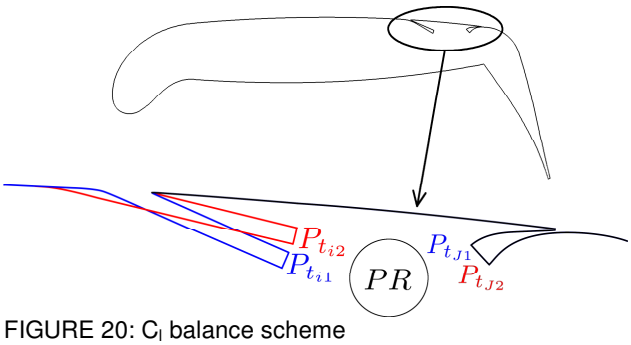

FIGURE 20: C_l balance scheme

According to figure 20 and using the geometry 1 as reference, the procedure is the following:

$$PR = \frac{P_{t_{J1}}}{P_{t_{i1}}}$$

$$P_{t_{J2}} = PR \cdot P_{t_{i2}}$$

$$\Rightarrow C_{\mu_1}(P_{t_{J1}}) \neq C_{\mu_2}(P_{t_{J2}})$$

The balanced C_l is then obtained by applying the new total pressure as boundary condition inside the jet plenum.

In the following the balance procedure is applied to the results obtained by the different geometries described previously. As a reference configuration for the balance, the geometry with β=10°, γ=0°, x=61%c is used.

The C_l balance applied to the results of the internal shape analysis is presented in table 4 and resumed in Figure 21. The effect of the balance becomes more important for high diffusion angles, since the pressure recovery is affected by the high positive pressure gradient along the duct. These cases present a lower total pressure at the end of the duct, which reduces the jet momentum coefficient. The most effective configuration is the one that provides the highest balanced lift coefficient, and results to be obtained with the parameters: β=10°, γ=3°, x=61%c.

	$C_{l,max}$	P_{ti}/P_∞	$C_{\mu,bal}$	$C_{l,max,bal}$
β=10°, γ=0°	5.342	0.9664	0.0356	5.342
β=10°, γ=3°	5.364	0.9652	0.0355	5.358
β=10°, γ=5°	5.372	0.9578	0.0349	5.328
β=10°, γ=6°	5.375	0.9348	0.0328	5.214
β=10°, γ=7°	5.376	0.8548	0.0257	4.735
β=20°, γ=0°	5.354	0.9652	0.0355	5.348
β=20°, γ=3°	5.364	0.9649	0.0355	5.356
β=20°, γ=5°	5.369	0.9615	0.0351	5.344
β=20°, γ=6°	5.371	0.9556	0.0346	5.316
β=20°, γ=7°	5.373	0.9371	0.0330	5.224

TABLE 4: Balance of the tested internal geometries, x=61%c

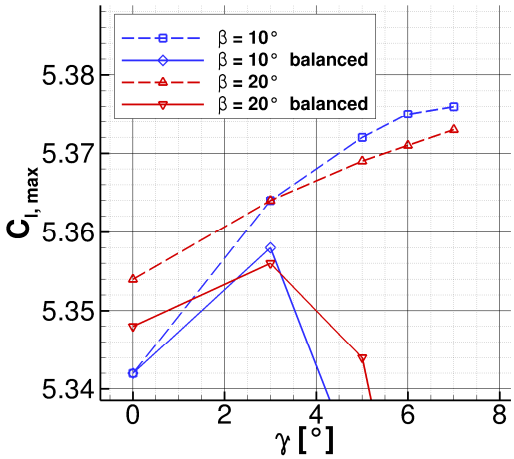

FIGURE 21: Balanced performances for the internal shape analysis

Following the same procedure, also the results obtained by sucking at different locations have been compared, as shown in table 5 and Figure 22. The highest total pressure is achieved at the end of the duct positioned at 85% of the airfoil chord, thanks to the suction at the location of highest dynamic pressure on the airfoil. However, also translating this higher duct pressure into a higher jet momentum, the lift coefficient remains lower than the one achieved by two other locations. The most effective location is 30% of the chord length, even though the pressure recovery is lower than for the two other cases. In Figure 22 one can see the effect of the balance, that reduces significantly the differences in $C_{l,max}$ without changing the trend.

	$C_{l,max}$	P_{ti}/P_∞	$C_{\mu,bal}$	$C_{l,max,bal}$
x = 30%c	5.620	0.9302	0.0324	5.435
x = 61%c	5.342	0.9664	0.0356	5.342
x = 85%c	4.982	1.0016	0.0387	5.245

TABLE 5: Balance of the tested locations, β=10° and γ=0°

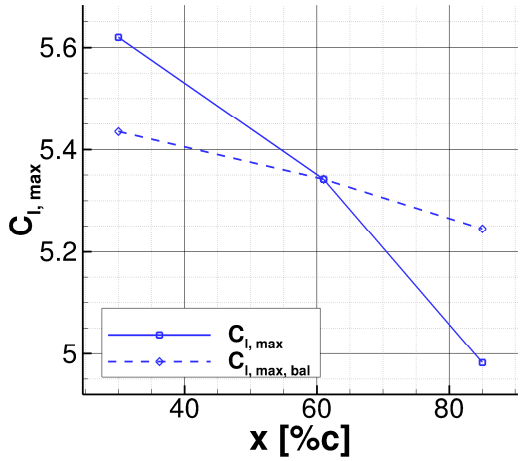

FIGURE 22: Balanced performances for the location analysis

5. RESPONSE TO VARIATIONS OF C_μ AND α

The configuration characterized by β=10°, γ=0°, x=61%c has been also tested with different jet momentum coefficients, and compared with results previously obtained without suction. The increase of $C_{l,max}$ and stall angle of attack are present in the whole range of C_μ tested here. The stall behavior is not affected by suction, as shown in Figure 23. It appears that the trend of α_{stall} is similar to the one that characterizes the configuration with droopnose and no suction.

The same suction device has been tested on a configuration not equipped with leading-edge protection. In this case, as shown in both Figure 23 and 24, the benefit of suction is much lower. For C_μ=0.0356, the maximum lift coefficient of the droopnose configuration is increased by about 6.5% due to suction, whereas with the clean nose the increase is only of 3%. Also the stall angle of attack is more sensitive to suction in presence of the leading edge device, increasing of 2.75° in the case of droopnose and only 0.5° with clean nose.

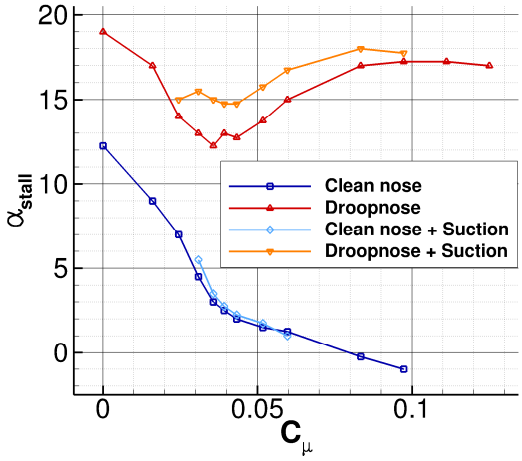

FIGURE 23: Effect of C_μ on the stall angle of attack

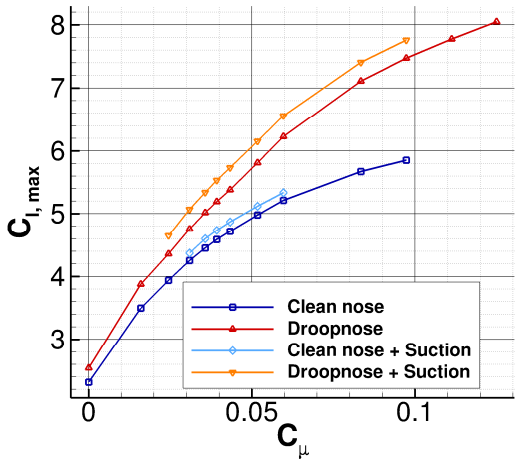

FIGURE 24: Effect of C_μ on the maximum lift coefficient

6. AERODYNAMIC COEFFICIENTS

Table 6 shows the large improvements that have been achieved using the carefully designed leading-edge protection device and wall suction. The suction slot configuration chosen for this comparison is again the one used as reference for the previous analyses: β=10°, γ=0°, x=61%c. All the data reported in the table refer to the trailing-edge configuration described in Chapter 2. The benefit of both the droopnose devices and the wall suction is to reduce the required blowing power, and to increase the angle of attack of maximum lift coefficient. As shown in table 6, a target $C_l \approx 4.7$ can be obtained with about 28% less jet momentum thanks to the droopnose, which becomes about 40% if the wall suction is also implemented. As a consequence, the lift gain factor is increased of the same proportion, reaching 114.5 for low blowing rates, as one can see in Figure 25. Note that the droopnose and suction approaches have been so far tested only for one flap setting: deflection angle of 65°. Analyses performed with the clean nose configuration showed that higher lift gain factor may be achieved with a lower deflection, at around 50°. Therefore it is reasonable to expect a further increase of the lift gain factor when droopnose and wall suction are applied with a lower flap deflection angle. Analyses in this direction are currently in progress. It is important to note that the stall angle of attack in this lift range is brought to values suitable for landing and take off operations: from 2° to 13° for the droopnose and to 17° for both droopnose and suction.

The pitching moment represents an important issue for the stability of the aircraft, and due to an improved load distribution along the chord, and the lower jet momentum requirement, the pitching moment is improved by about 16% by the droopnose and 33% with also the effect of the suction.

	C_μ	α[°]	C_l	C_d	C_m
Clean nose	0.0433	2.0	4.719	0.0719	-0.808
Droopnose	0.0309	12.0	4.719	0.0784	-0.677
Droopnose + suction	0.0245	17.0	4.663	0.0874	-0.544

TABLE 6: Aerodynamic coefficients achieved by leading-edge protection and wall suction

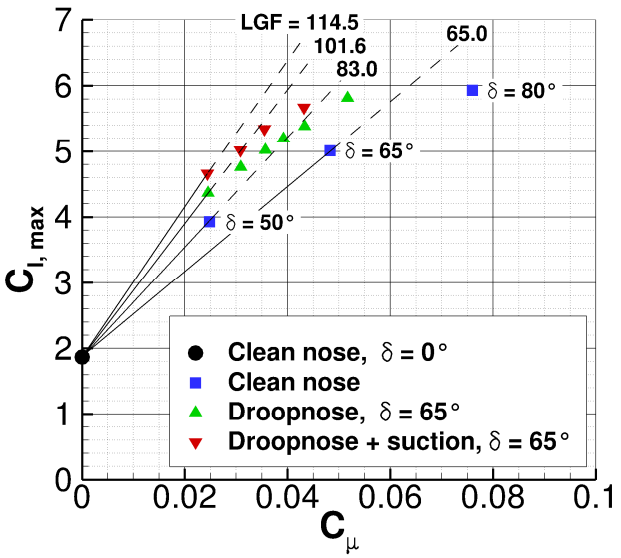

FIGURE 25: Evolution of the lift gain factor due to different high-lift devices

7. CONCLUSIONS

The present work reports on the progress of the new technologies developed within the framework of the Collaborative Research Centre SFB880. The potentials of wall suction, needed to generate an airstream to the compressors that supply the active flap, are assessed. The improvement of the flow over the suction side of the airfoil, made possible by the wall suction, allows significant improvements in the behavior of the airfoil at high angles of attack. The effect is to reduce the needed blowing power and to increase the angle of attack of maximum lift coefficient. A lift coefficient of about 4.7 can be achieved with 16% less blowing momentum, with respect to the same configuration without suction. The maximum angle of attack is increased from 12.0° to 17.0° due to suction.

Different suction-slot geometries and locations have been investigated, yielding physical insight on wall suction interactions with the flow around the airfoil. The study highlights the high efficiency of suction downstream of the low pressure area at the nose. Positioning the slot in this critical area brings higher circulation and appears to be more effective than wall suction close to the blowing jet. Using suction on the flap surface to avoid flow separation in presence of low jet momentum is not an effective solution, because of the complex flow dynamics over the flap at high angles of attack.

An approach is proposed to compare and evaluate slot geometries and locations taking into account both the aerodynamic performance of the airfoil and the total pressure recovery inside the duct.

Finally wall suction is found to be about twice as effective when applied in presence of a droopnose leading-edge device, rather than the clean nose configuration.

In the future the expertise gained during the present work will be employed to design a 3D model of the inlet slot that will lead air to the compact compressors. In this context

3D computations will take into account other constrains due to 3D geometry requirements.

ACKNOWLEDGEMENT

The funding of this work of the Collaborative Research Centre SFB 880 by the German Research Foundation, DFG, is thankfully acknowledged.

REFERENCES

[1] Werner-Spatz, C.; Heinze, W.; Horst, P.; Radespiel, R.: *Multidisciplinary Conceptual Design for Aircraft with Circulation Control High-Lift Systems*. CEAS Aeronautical Journal, Vol. 3, pp. 145-164, 2012.

[2] Radespiel, R., Pfingsten, K.-C., Jensch, C.: *Flow Analysis of Augmented High-Lift Systems*. In: Radespiel, R., Rossow, C.-C., Brinkmann, B. (Eds.): Hermann Schlichting - 100 Years. Scientific Colloquium Celebrating the Anniversary of his Birthday, Braunschweig, Germany 2007. Notes on Numerical Fluid Mechanics and Multidisciplinary Design, Vol. 102, Springer-Verlag, ISBN 978-3-540-95997-7, 2009.

[3] Jensch, C., Pfingsten, K. C., Radespiel, R., Schuermann, M., Haupt, M., and Bauss, S.: *Design Aspects of a Gapless High-Lift System with Active Blowing*, DLRK 2009, Aachen, 2009.

[4] Jensch, C., Pfingsten, K. C., and Radespiel, R.: *Numerical Investigation of Leading Edge Blowing and Optimization of the Slot and Flap Geometry for a Circulation Control Airfoil*, Notes on Numerical Fluid Mechanics and Multidisciplinary Design, Vol. 112, Springer Verlag, 2010.

[5] Pfingsten, K. C., Jensch, C., Körber, K. V., and Radespiel, R.: *Numerical simulation of the flow around circulation control airfoils*, First CEAS European Air and Space Conference, Berlin, 2007.

[6] Burnazzi, M., and Radespiel, R.: *Design of a Droopnose Configuration for a Coanda Active Flap Application*, 51th AIAA Aerospace Sciences Meeting, Dallas (TX), AIAA 2013-0487.

[7] Wild, J.: *Experimental investigation of Mach- and Reynolds-number dependencies of the stall behavior of 2-element and 3-element high-lift wing sections*, 50st AIAA Aerospace Sciences Meeting, Nashville (TN), AIAA 2012-108

[8] Swanson, R.C., Rumsey, C.L.: *Computation of circulation control airfoil flows*. Computers and Fluids, Vol. 38, 2009, pp. 1925-1942.

[9] Pfingsten, K. C., Cecora, R. D., and Radespiel, R.: *An experimental investigation of a gapless high-lift system using circulation control*, Katnet II Conference, Bremen, 2009.

[10] Beck, N., Wentrup, M., and Radespiel, R.: *Realisierung eines Windkanalexperiments für Aktiven Hochauftrieb*, DLRK2011_241373, 2011.

[11] Kroll, N., Rossow, C.-C., Schwamborn, D., Becker, K., and Heller, G.: *MEGAFLOW - A Numerical Flow Simulation Tool for Transport Aircraft Design*, ICAS Congress, Toronto, 2002.

[12] Schwamborn, D., Gerhold, T., and Heinrich, R.: *The DLR TAU-Code: Recent applications in Research and Industry*, ECCOMAS CFD, Egmond aan Zee, The Netherlands, 2006.

[13] Pfingsten, K. C., and Radespiel, R.: *Experimental and numerical investigation of a circulation control airfoil*, 47th AIAA Aerospace Sciences Meeting, Orlando, AIAA 2009-533.

[14] Shur, M. L., Strelets, M. K., Travin, A. K., and Spalart, P. R.: *Turbulence Modeling in Rotating and Curved Channels: Assessing the Spalart-Shur Correction*, AIAA Journal, Vol. 38, pp. 784-792, 2000.